Recycled ancient ghost carbonate in the Pitcairn mantle plume

Xiao-Jun Wang[a], Li-Hui Chen[a,1], Albrecht W. Hofmann[b,1], Takeshi Hanyu[c], Hiroshi Kawabata[d], Yuan Zhong[a], Lie-Wen Xie[e], Jin-Hua Shi[a], Takashi Miyazaki[c], Yuka Hirahara[c,2], Toshiro Takahashi[c,3], Ryoko Senda[c,4], Qing Chang[c], Bogdan S. Vaglarov[c], and Jun-Ichi Kimura[c]

[a]State Key Laboratory for Mineral Deposits Research, School of Earth Sciences and Engineering, Nanjing University, 210023 Nanjing, China; [b]Abteilung Klimageochemie, Max-Planck-Institut für Chemie, D-55128 Mainz, Germany; [c]Department of Solid Earth Geochemistry, Japan Agency for Marine-Earth Science and Technology, 237-0061 Yokosuka, Japan; [d]Faculty of Science and Technology, Kochi University, 780-8520 Kochi, Japan; and [e]State Key Laboratory of Lithospheric Evolution, Institute of Geology and Geophysics, Chinese Academy of Sciences, 100029 Beijing, China

Edited by Richard W. Carlson, Carnegie Institution for Science, Washington, DC, and approved July 17, 2018 (received for review November 9, 2017)

The extreme Sr, Nd, Hf, and Pb isotopic compositions found in Pitcairn Island basalts have been labeled enriched mantle 1 (EM1), characterizing them as one of the isotopic mantle end members. The EM1 origin has been vigorously debated for over 25 years, with interpretations ranging from delaminated subcontinental lithosphere, to recycled lower continental crust, to recycled oceanic crust carrying ancient pelagic sediments, all of which may potentially generate the requisite radiogenic isotopic composition. Here we find that δ^{26}Mg ratios in Pitcairn EM1 basalts are significantly lower than in normal mantle and are the lowest values so far recorded in oceanic basalts. A global survey of Mg isotopic compositions of potentially recycled components shows that marine carbonates constitute the most common and typical reservoir invariably characterized by extremely low δ^{26}Mg values. We therefore infer that the subnormal δ^{26}Mg of the Pitcairn EM1 component originates from subducted marine carbonates. This, combined with previously published evidence showing exceptionally unradiogenic Pb as well as sulfur isotopes affected by mass-independent fractionation, suggests that the Pitcairn EM1 component is most likely derived from late Archean subducted carbonate-bearing sediments. However, the low Ca/Al ratios of Pitcairn lavas are inconsistent with experimental evidence showing high Ca/Al ratios in melts derived from carbonate-bearing mantle sources. We suggest that carbonate–silicate reactions in the late Archean subducted sediments exhausted the carbonates, but the isotopically light magnesium of the carbonate was incorporated in the silicates, which then entered the lower mantle and ultimately became the Pitcairn plume source.

Pitcairn mantle plume | EM1 | magnesium isotopes | ancient carbonate-bearing sediments

The geochemical and isotopic diversity of ocean island basalts (OIBs) erupted at hot spots is generated by partial melting of heterogeneous mantle sources that contain recycled crustal and/or lithospheric mantle materials (1, 2). Specific recycled components generally show radiogenic isotope ratios distinct from the ambient mantle, and radiogenic isotopes are therefore widely used tools for tracing them. However, this tool can be compromised by the fact that similar radiogenic isotope features can appear in different geological reservoirs. Thus, the exceptionally unradiogenic Pb isotopes observed in intraplate enriched mantle 1 [EM1 (3)] lavas have been variously attributed to recycled ancient pelagic sediments (4–7), subducted oceanic plateau (8), recycled lower continental crust (LCC) (9), delaminated subcontinental lithospheric mantle (10), and recycled mafic sediments (11). Fortunately, a combination of stable and radiogenic isotopes can sometimes be used to discriminate the nature of recycled materials less ambiguously. Recently, Delavault et al. (7) demonstrated the presence of sulfur isotopes affected by mass-independent fractionation in sulfides contained by Pitcairn lavas, which are likely to have been introduced into the Pitcairn source by subduction of ancient sediments. Here we use a stable isotope tracer, magnesium, which undergoes strong isotopic fractionation during precipitation of carbonate from seawater/pore fluids (12), producing distinctively low δ^{26}Mg values in marine carbonates. Because of this, it appears to be an excellent tracer of a more specific recycled component than, for example, oxygen isotopes.

There are many models for the creation of chemical heterogeneity in the source regions of OIBs that invoke the recycling of oceanic crust and lithologically different sediments through the mantle (5, 13–15). The existing Mg isotope data show that marine sediments and altered oceanic crust have variable Mg isotopic signatures that differ significantly from those of normal peridotitic mantle (Fig. 1). In particular, marine carbonates stand out by their extremely light Mg isotopes, reaching values of δ^{26}Mg as low as −5‰. This provides the opportunity to use anomalous Mg isotopic signatures in erupted OIBs as tracers of their sources. A recent Mg isotopic study on Hawaii and Louisville basalts presented a first test of this proposition, showing small but significant differences in δ^{26}Mg (16). However, the current Mg isotope database for OIBs is still very small, and the Mg isotope characteristics of the several classical mantle species, i.e., HIMU (high $\mu = {}^{238}U/{}^{204}Pb$), EM1, and enriched mantle 2 (3), remain to be evaluated. Here we focus

Significance

Lavas from Pitcairn Island are the best candidates for exploring the origin of the enigmatic EM1 component found in some mantle plumes because they show the most extreme isotopic compositions of Sr, Nd, Hf, and Pb that define the EM1 component. We find that these lavas have the lowest δ^{26}Mg values so far recorded in oceanic basalts. Subducted late Archean dolomite-bearing sediments are the most plausible source of the low-δ^{26}Mg feature of Pitcairn lavas. This requires that an ancient, originally sedimentary component has been emplaced near the core–mantle boundary to ultimately become part of the Pitcairn plume source.

Author contributions: X.-J.W. and L.-H.C. designed research; X.-J.W., L.-H.C., A.W.H., T.H., H.K., Y.Z., L.-W.X., J.-H.S., T.M., Y.H., T.T., R.S., Q.C., B.S.V., and J.-I.K. performed research; X.-J.W., L.-H.C., A.W.H., T.H., and H.K. analyzed data; and X.-J.W., L.-H.C., A.W.H., and T.H. wrote the paper.

The authors declare no conflict of interest.

This article is a PNAS Direct Submission.

[1]To whom correspondence may be addressed. Email: chenlh@nju.edu.cn or albrecht.hofmann@mpic.de.

[2]Present address: Chiba Institute of Technology, 275-0016 Narashino, Japan.

[3]Present address: Department of Geology, Niigata University, 950-2181 Niigata, Japan.

[4]Present address: Faculty of Social and Cultural Studies, Kyushu University, 819-0395 Fukuoka, Japan.

This article contains supporting information online at www.pnas.org/lookup/suppl/doi:10.1073/pnas.1719570115/-/DCSupplemental.

Published online August 13, 2018.

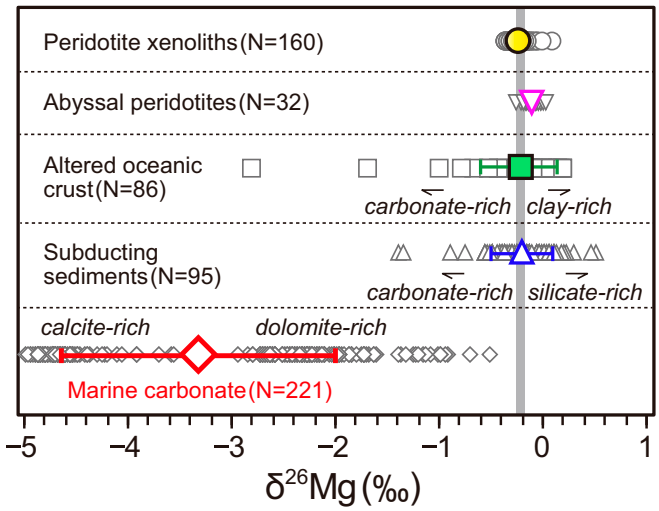

Fig. 1. Mg isotopic compositions of mantle rocks and some potentially recycled components. The average δ^{26}Mg value, the SD (1 SD), and the number of samples (N) are given for each reservoir. For peridotite xenoliths and abyssal peridotites, the error bars are covered by the symbols for the average values. The vertical gray bar represents the δ^{26}Mg range of peridotitic mantle [−0.23 ± 0.04‰ (20)]. See *SI Appendix, Part 3* for data sources.

on the EM1 end member by presenting whole-rock Mg isotopic analyses of Rarotonga and Pitcairn Island lavas. The combination of Mg isotopes with Sr–Nd–Hf–Pb isotopes provides critical evidence for the return of ancient, subducted dolomite-derived magnesium in EM1 lavas erupted at Earth's surface.

Pitcairn mantle plume has recently been identified as a category 1–primary plume, by French and Romanowicz (17), who used waveform seismic tomography to trace it down to the core–mantle boundary. Identifying the nature and age of surface-derived geochemical signatures in such a plume therefore provides important constraints on the nature and time scale of deep mantle circulation processes.

Results

We analyzed 12 samples from Pitcairn Island (*SI Appendix*, Fig. S1). Seven of the samples come from the shield-building Tedside volcanics, and five others are from the late-stage, posterosional volcanics including Pulawana, Christians Cave Formation, and Adamstown volcanics. Duncan et al. (18) reported K-Ar ages for Tedside and late-stage volcanics of 0.95–0.76 and 0.67–0.45 Ma, respectively. The whole-rock Mg isotopic compositions, and newly measured major and trace elements, as well as the Sr–Nd–Hf–Pb isotope ratios are reported in Datasets S1–S3. For comparison, we also analyzed Mg isotopes of four well-characterized samples (19) from Rarotonga Island (*SI Appendix*, Fig. S1), which show Sr–Nd–Hf–Pb isotope ratios trending toward the EM1 end member (5, 19). All of our samples belong to the alkaline series, and most of them are relatively unevolved rocks with SiO_2 < 52 wt % (*SI Appendix*, Fig. S2). The Tedside basalts have robust EM1 end member isotopic signatures compared with the late-stage Pitcairn lavas and Rarotonga basalts (*SI Appendix*, Fig. S3).

The δ^{26}Mg values of Tedside basalts range from −0.40 to −0.31‰, clearly lower than those of the late-stage Pitcairn lavas (−0.30 to −0.16‰), peridotitic mantle [δ^{26}Mg = −0.23 ± 0.04‰ (20) or δ^{26}Mg = −0.25 ± 0.04‰ (21)], and other typical OIBs (Hawaii, Louisville, and Rarotonga) (Fig. 2). The lower end of the Pitcairn range is the lowest value observed so far in OIBs (see the compilation in ref. 21) and is close to the upper bound of the continental intraplate EM1 end member basalts from Wudalianchi and Erkeshan [hereafter referred to as "intracontinental EM1 basalts"; δ^{26}Mg = −0.57 to −0.45‰ (22, 23)] in northeast China (Fig. 3). The δ^{26}Mg values of Pitcairn and Rarotonga EM1 basalts, taken together, exhibit significant negative correlations with $^{87}Sr/^{86}Sr$ and positive correlations with $^{206}Pb/^{204}Pb$, ε_{Nd}, and ε_{Hf} (Fig. 3). Inclusion of the intracontinental EM1 basalts strengthens these correlations and further extends their range to even lower δ^{26}Mg values. A common heritage of oceanic and continental EM1 magmas is further substantiated by the correlation between δ^{26}Mg and CaO/Al_2O_3 (Fig. 4). Oceanic EM1 lavas exhibit the lowest CaO/Al_2O_3 ratios within the global OIB association (24), and the intracontinental EM1 basalts have even lower CaO/Al_2O_3 ratios. Therefore, we consider all these EM1-type intraplate lavas as a group to explore the origin of the characteristic EM1 component.

Discussion

Subnormal δ^{26}Mg of the EM1 Mantle Sources. The analyzed OIB samples are fresh, and no secondary carbonates can be observed (*SI Appendix*, Fig. S4). Their loss on ignition (LOI) values are very low (mostly <1.0 wt %; Dataset S2), and there is no correlation between δ^{26}Mg and LOI, precluding any obvious chemical weathering. Seawater has lower δ^{26}Mg [−0.83‰ (21)] value than reported values of OIBs (16, 21); thus, seawater contamination might potentially modify the Mg isotopic composition of OIBs. However, seawater has much lower Mg concentrations [0.128 wt % (25)] than our basalt samples with low δ^{26}Mg values, and more than 90% of seawater would have to be added to the basalt to shift the δ^{26}Mg of basalt from −0.25 to −0.40‰. This can be ruled out because of the low LOI of our samples. Hence, the low δ^{26}Mg values of Tedside basalts are unlikely to be the result of postmagmatic alteration.

Fractionation of olivine, pyroxene, and plagioclase dominate the major element variations of Pitcairn lavas with MgO >4 wt %, and fractionation of Fe-Ti–rich phases (e.g., ilmenite) is apparent in lavas with MgO <4 wt % (*SI Appendix*, Fig. S2). Fractionation of the former group of phases can induce very minor [<0.07‰ (26)] Mg isotope fractionation, but that of the latter may lead to considerable fractionation (27). Therefore, because Mg isotopic variation in the two highly evolved samples (MgO < 3 wt %; Fig. 2) might be largely controlled by fractionation of Fe-Ti–oxides, we ignore these samples hereafter. Overall, crystal fractionation cannot be responsible for lowering δ^{26}Mg values, because the lowest δ^{26}Mg (−0.40‰) values appear in high-MgO (>8 wt %) Tedside samples, and these should reflect the inherent properties of the primary magmas. For Rarotonga lavas, their high MgO

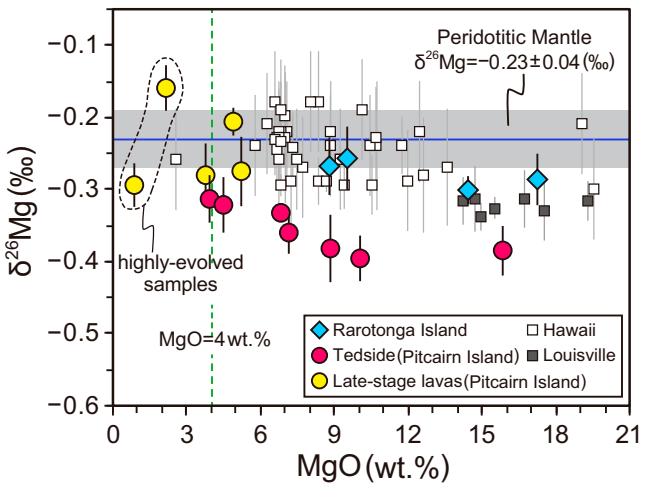

Fig. 2. δ^{26}Mg versus MgO for the Pitcairn Island and Rarotonga samples. Also shown are published data (16, 59) for other OIBs. The subnormal δ^{26}Mg character of the Tedside lavas from Pitcairn is clear. Error bars on δ^{26}Mg represent 2 SD uncertainties.

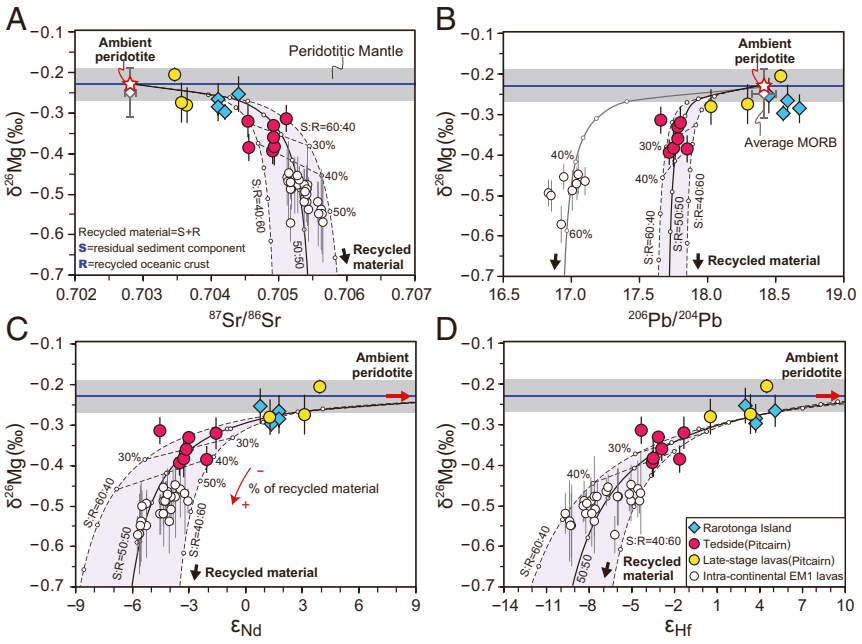

Fig. 3. δ^{26}Mg versus (*A*) $^{87}Sr/^{86}Sr$, (*B*) $^{206}Pb/^{204}Pb$, (*C*) ε_{Nd}, and (*D*) ε_{Hf} isotopic arrays for mixing of ambient peridotite and recycled material. Recycled material is the mix of recycled oceanic crust (R) and residual sediment component (S) in various mixing proportions. For details of how the composition of the residual sediment component (S) is derived, see *Discussion* and *SI Appendix, Part 2*. Mixing curves are marked in 10% increments. An enlarged figure (*SI Appendix*, Fig. S6) showing mixtures of all of the three end members is given in *SI Appendix*. The modeling parameters can be found in *SI Appendix*, Table S1. Also plotted are data for intracontinental EM1 basalts (see *SI Appendix, Part 3* for data sources). A separate mixing curve for these lavas is required in *B* because the estimated age and μ ($^{238}U/^{204}Pb$) value (22) of the subducted sediments that evolved into the EM1 component in their source are different from those of the Pitcairn EM1 component (7). For average MORB, the δ^{26}Mg value (−0.25 ± 0.06‰, 2 SD) is from ref. 59, and radiogenic isotope ratios are the mean (±95% confidence interval on the mean) given in ref. 33. Others are as in Fig. 2.

contents (Fig. 2 and *SI Appendix*, Fig. S2) indicate that their normal mantle-like δ^{26}Mg values are those of the respective primary melts. Isotope fractionation during partial melting also cannot produce the low-δ^{26}Mg feature of Tedside samples, because the largest δ^{26}Mg difference between partial melts and solid residue is less than 0.1‰, no matter whether the initial source is a garnet pyroxenite or a peridotite (16). In summary, neither crystallization nor partial melting effects can explain the observed low δ^{26}Mg values (as low as −0.40‰) in EM1-type OIBs, and the subnormal δ^{26}Mg lavas require an isotopically light mantle source component, as was also the case for the intracontinental EM1 basalts (22). Given the correlations between δ^{26}Mg and Sr–Nd–Hf–Pb isotopes of EM1 lavas (Fig. 3), we conclude that the unradiogenic isotope ratios of Pb, Nd, and Hf, together with the elevated $^{87}Sr/^{86}Sr$ ratios, are all coupled with subnormal δ^{26}Mg values in the EM1 component.

The Origin of EM1. The low δ^{26}Mg values of Pitcairn lavas are clearly at odds with some of the earlier models advocating delaminated subcontinental lithosphere or recycled LCC, given that neither of these reservoirs have primary subnormal δ^{26}Mg (21, 22). A summary of Mg isotope data for 160 global peridotite xenoliths that sample the subcontinental lithospheric mantle with various parageneses, chemical compositions, and ages definitely shows no evidence for subnormal δ^{26}Mg values that would qualify them as the EM1 source component (Fig. 1). Although some peridotite xenoliths have been extensively metasomatised by carbonatite or CO_2-rich silicate melts, they still maintain mantle-like δ^{26}Mg values [−0.27 to −0.16‰ (28)]. The δ^{26}Mg values of cratonic eclogites are highly heterogeneous and can be as low as −1.0‰ (29), and such rocks may thus potentially constitute a low-δ^{26}Mg origin. However, such eclogites are only a minor (<1 vol %) component of subcontinental lithospheric mantle (30). They are usually thought to represent the composition of recycled ancient oceanic crust (29, 31, 32). The reconstructed bulk compositions of these eclogites, as represented by the 2.9-Ga Lace basaltic eclogites, yield median Sm/Nd and Lu/Hf ratios of 0.40 and 0.27, respectively (32). These are higher than the average values of midocean ridge basalts (MORB) [Sm/Nd = 0.326 and Lu/Hf = 0.195 (33)]. Therefore, the long-term isotopic evolution of the cratonic eclogites in the mantle should lead to highly radiogenic Nd–Hf isotopic compositions (32) rather than the observed, unradiogenic EM1-type end member. A collection of LCC xenoliths that have not been affected by carbonate metasomatism indicates that normal LCC also has mantle-like δ^{26}Mg value [δ^{26}Mg = −0.26 ± 0.06‰ (34)], although a few of the intensively metasomatised low-MgO samples do have δ^{26}Mg values as low as −0.7‰ (34). Therefore, on balance, models invoking delaminated subcontinental lithosphere and/or LCC are difficult to reconcile with the consistently subnormal δ^{26}Mg of the EM1 sources.

Recycled ancient ocean plateau material, which contains cumulus gabbro, has also been suggested to be the origin of Pitcairn EM1 source (8). This possibility is inconsistent with the

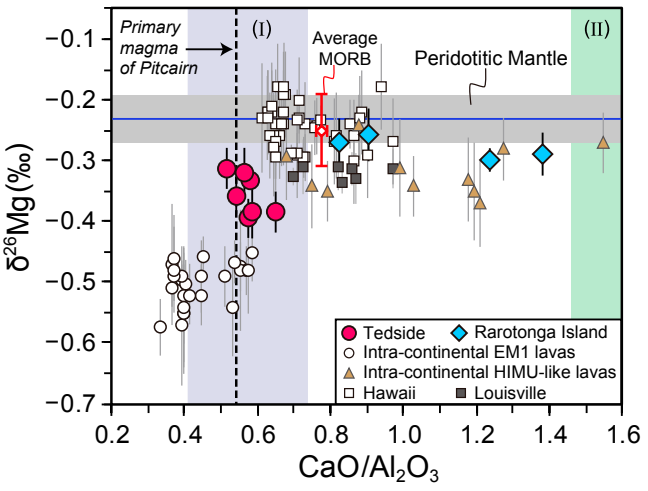

Fig. 4. Extreme EM1 lavas show exceptionally low CaO/Al_2O_3 and δ^{26}Mg values. The late-stage Pitcairn lavas are omitted here because their CaO/Al_2O_3 ratios have been severely modified by fractionation of clinopyroxene and plagioclase. Also plotted are literature data for other types of basalts (see *SI Appendix, Part 3* for data sources). Shaded regions labeled I (gray) and II (green) denote the CaO/Al_2O_3 ranges for experimental partial melts of pyroxenite (55, 56) and carbonated eclogite (44). For Pitcairn primary magmas, the CaO/Al_2O_3 ratio is from ref. 24; for average MORB, it is the calculated mean (±95% confidence interval on the mean) based on the data in ref. 33. Others are as in Fig. 3.

low-δ^{26}Mg feature of the Pitcairn EM1 source because Mg isotopic compositions of gabbros from both oceanic crust and ophiolite do not deviate from that of peridotitic mantle (35, 36). Similarly, recycled mafic sediments consist of olivine and pyroxene, and their weathering products (i.e., clay) (11) are not expected to satisfy the subnormal δ^{26}Mg signature of the Pitcairn EM1 component, because these minerals show mantle-like or even higher δ^{26}Mg values (21).

Recycled ancient pelagic sediments have repeatedly been invoked as EM1 mantle sources (4–7). This interpretation is supported here by the systematically lowered Nb/Th ratios and the positive correlations in the plots of ε_{Nd} and $^{206}Pb/^{204}Pb$ versus Nb/Th for Pitcairn Island basalts (*SI Appendix*, Fig. S5), which require some continental crust–derived, most likely sedimentary sources. In particular, the recent discovery of mass-independent fractionation of sulfur isotopes (S-MIF down to $\Delta^{33}S = -0.8‰$) in sulfides contained by Pitcairn lavas, along with three-stage Pb isotope growth modeling, has constrained the late Archean age (2.5–2.6 Ga) of the recycled sediments incorporated into the Pitcairn EM1 source (7). Our results are fully consistent with this interpretation, but they add an additional constraint that further specifies the nature of the recycled sediments. Thus, the recycled sediments must initially contain significant amounts of carbonates, to satisfy the low-δ^{26}Mg feature of Pitcairn EM1 component. Among potentially subducted materials, marine carbonates identify the low-δ^{26}Mg end member by their extremely light Mg isotopic compositions, which are remarkably distinct from other Mg reservoirs and peridotitic mantle (Fig. 1). Accordingly, marine carbonates with extremely low δ^{26}Mg values, especially for the Mg-rich carbonates (dolomite), appear to be the unique reservoir capable of dominating the Mg isotopic compositions of bulk sediments. Because the metamorphic equivalents of the subducted sediments tend to preserve their original Mg isotopic compositions (37), recycled Archean dolomite-bearing sediments provide a likely origin of the low-δ^{26}Mg feature of EM1 component. In the following sections, we discuss additional aspects of this proposition.

Archean Carbonate Deposits. How common are marine carbonate deposits in Archean time? Veizer et al. (38) reviewed the geochemistry of Archean carbonates with geological attributes of marine sediments and noted that they are "a minor component of the Archean greenstone belts." Nevertheless, they do occur in many such greenstone belts, including the Yellowknife Supergroup; the Abitibi, Michipicoten, Uchi, and Wabigoon Greenstone Belts in Canada; the Main Greenstone Belt of Zimbabwe; the Sargur Marbles of India; the Warrawoona Group of Australia (38, 39); and the Neoarchean Transvaal carbonate platform, South Africa (40). Most of these deposits appear to have been originally formed as aragonitic limestones, but many have been replaced by dolomite and/or ankerite during sedimentation and diagenesis (38, 41), thus constituting a significant Mg reservoir with isotopically light magnesium. We conclude that although such carbonates may indeed be minor constituents of Archean sedimentary sequences, they are by no means uncommon. In this context, it is important to remember that extreme EM1 end member basalts are also rare in the oceanic basalt family.

Ghost Carbonate in the Pitcairn Source. Another question is, how was the isotopically light Mg of dolomite in originally subducted sediments introduced into the EM1 source? One possible way is that the bulk subducted dolomite, together with its surrounding silicate sediments, was directly incorporated into the Pitcairn EM1 source. However, this can be largely ruled out by the major element compositions of Pitcairn EM1 lavas. These lavas are characterized by the lowest CaO and CaO/Al_2O_3 ratios but among the highest SiO_2 contents in the global OIB database (24, 42, 43). Their low CaO/Al_2O_3 ratios (0.5–0.6) are not induced by extensive fractionation of clinopyroxene and plagioclase, and the estimated CaO/Al_2O_3 ratio of their primary melts is as low as 0.54 (24). By contrast, experimental work has shown that partial melting of carbonate-bearing mantle rocks (peridotite/pyroxenite) produces melts with high CaO and low SiO_2 contents (44, 45). Notably, the HIMU-like low-δ^{26}Mg basalts from New Zealand, which were suggested to derive from a carbonated eclogite source (28), show extremely high CaO/Al_2O_3 and low SiO_2 (Fig. 4 and ref. 46), features that are distinct from the low-δ^{26}Mg EM1 basalts. Accordingly, the low CaO and CaO/Al_2O_3 of Pitcairn lavas are inconsistent with the presence of carbonate in the direct mantle source. An alternative possibility is that the isotopically light Mg remains in the EM1 source as a "ghost" of the originally subducted dolomite, but the carbonate component of the dolomite has been lost. This is somewhat analogous to the interpretations of Hawaii and Mangaia hot spot lavas, where it has been shown that the original chemical or isotopic identity of recycled crustal materials may be present only as a ghost or phantom signature in the mantle source, whereas their actual lithological identity has been completely lost (47, 48). In the present case, a prerequisite is that the isotopically light Mg of dolomite in the originally subducted sediments must be inherited by Mg-silicate and then be incorporated into the EM1 source. Below, we discuss possible mechanisms for such processes.

Possible Decarbonation Mechanisms. As suggested above, the low-δ^{26}Mg feature of Pitcairn EM1 component is inferred to be derived from dolomite in Archean subducted sediments. Because the Archean subduction zones are hot, such sediments are prone to losing their carbon inventory during subduction, through carbonate melting or subsolidus decarbonation (49). According to experimentally determined solidi (50), carbonate-bearing sediments may possibly melt within the pressure range of 6–9 GPa in hot subduction zones. Because the carbonatite melts produced by melting of carbonate-bearing sediments in the pressure range of 6–9 GPa are Ca-rich and Mg-poor (50), most of the dolomite-derived Mg budget will remain in the silicate residue after melt extraction. Therefore, the original low-δ^{26}Mg signature is expected to be transferred to the silicate residue, thus providing one possible solution to the ghost carbonate Mg isotopic signature of the Pitcairn EM1 source. However, the extraction of carbonatite melts from subducted dolomite-bearing sediments would also remove large proportions of incompatible trace elements, and this should deplete the residual source in incompatible trace elements to such an extent that it would no longer be capable of generating highly trace element-enriched (Pitcairn-type) basalts. Therefore, carbonate melting is not a suitable decarbonizing mechanism to generate the particular EM1 source of Pitcairn lavas.

Another plausible mechanism is decarbonation reaction during subduction. The dolomite-bearing sediments are SiO_2-rich, and they will be transformed into assemblages mainly consisting of dolomite + quartz/coesite at intermediate depths [<~150 km (50)] or magnesite + coesite at greater depths [>~150 km (50)]. During subduction of these assemblages, the following decarbonation reactions will easily occur under suitable P–T–fO_2 conditions (51–53):

$$CaMg(CO_3)_2\ (\text{dolomite}) + 2SiO_2\ (\text{coesite}) \rightarrow CaMgSi_2O_6\ (\text{diopside}) + 2CO_2 \quad [1]$$

$$CaMg(CO_3)_2\ (\text{dolomite}) + 2SiO_2\ (\text{coesite}) \rightarrow CaMgSi_2O_6\ (\text{diopside}) + 2C(\text{graphite/diamond}) + 2O_2 \quad [2]$$

$$MgCO_3\ (\text{magnesite}) + SiO_2\ (\text{coesite}) \rightarrow MgSiO_3\ (\text{enstatite}) + CO_2. \quad [3]$$

Through these reactions, the silicate products (diopside and enstatite) can accommodate the Mg released by carbonate reactants, providing a feasible mechanism whereby the light Mg isotopic compositions of the original dolomite can be inherited by silicate

products to form an isotopically light silicate component (21). Meanwhile, incompatible elements, including rare earth elements, can also be hosted in the silicate products, e.g., diopside. This silicate residue, bearing a ghost carbonate Mg isotopic signature inherited from the subducted carbonate, will ultimately become the plume source for the Pitcairn EM1 magmas.

Quantitative Evaluation of the Subducted Carbonate. A three-component mixture of ancient sediment, old recycled oceanic crust, and ambient mantle peridotite has been suggested to constitute the Pitcairn mantle source by several previous studies proposing sediment recycling (4–7). Based on the Mg isotopic constraint in this study, we suggest that the ancient sediment component is the silicate residue of Archean (~2.5 Ga) subducted dolomite-bearing sediments after dolomite was completely decarbonated during subduction (hereafter referred to as "residual sediment component"). Here the proportion of dolomite ($\delta^{26}Mg = -2.68‰$; *SI Appendix*, Table S1) in originally subducted sediments is assumed to be as high as 50%, so as to provide sufficient isotopically light Mg to affect the Pitcairn source. Thus, the residual sediment component has evolved from a late Archean (~2.5 Ga) mixture initially consisting of 50% of dolomite and 50% of silicate sediments. To constrain the amount of originally subducted dolomite, we quantitatively modeled the mixing of ambient peridotite, recycled oceanic crust, and residual sediment component (Fig. 3 and *SI Appendix*, Fig. S6; see *SI Appendix*, *Part 2* for details). However, we find that the unmodified mixture of dolomite and clastic sediment would not generate present-day isotopic compositions (*SI Appendix*, Table S1) consistent with the Pitcairn isotopic data (e.g., $^{87}Sr/^{86}Sr$). We assume that this inconsistency is the result of trace element mobilization during subduction, and we therefore modified the trace element concentrations and parent/daughter isotopic ratios of the original mixture to obtain an appropriate residual sediment component whose isotopic compositions fit the mixing arrays in Fig. 3 and *SI Appendix*, Fig. S6. The final geochemical composition of the residual sediment component at ~2.5 Ga (*SI Appendix*, Table S1) was determined by mixing the chemical and isotopic compositions of ~2.5-Ga dolomites and ~2.5-Ga silicate sediments and then removing a fraction of the total trace element budget (see *SI Appendix*, *Part 2* for the detailed proportions of the removed part). After long-term (~2.5 Gyr) isolated isotopic evolution, this sediment component can generate the extreme Pitcairn EM1 component. Considering the high uncertainty of the element fractions mobilized during dehydration/melting of subducting slabs (54), we argue that the modification of the trace element concentrations of the above mixture and the mixing modeling is reasonable. According to the modeling results (Fig. 3), the proportion of recycled materials (oceanic crust + sediment) in the Pitcairn source is about 3–36%, and the corresponding percentage of the residual sediment component varies from ~1.5 to 18%. This means that the maximum amount of originally subducted dolomite ($\delta^{26}Mg = -2.68‰$) required to generate the low $\delta^{26}Mg$ value of the Pitcairn source is ~9%.

A new question arises whether the addition of CaO, inherited from the decomposed carbonate, to the Pitcairn source might increase the CaO/Al_2O_3 ratio of the Pitcairn lavas. A striking feature of the Pitcairn EM1 basalts is their exceptionally low CaO/Al_2O_3 ratios (Fig. 4). These are lower than the respective ratios found in MORB, in other types of OIBs, and in intracontinental HIMU-like basalts, and thus, they point to a pyroxenitic rather than peridotitic or carbonated eclogitic source lithology (Fig. 4; see also refs. 24, 55, and 56). Thus, we can answer the above question by estimating the effect of adding CaO released by ~9% of originally subducted dolomite to a pyroxenite on the final melt composition produced by melting of this mix. In the absence of specific experiments addressing this question, we have approached the problem using pMELTS (57) (for detail, see *SI Appendix*, Fig. S7). The major element compositions of the mixed lithology were calculated by mixing of 91% of the chemical compositions of the MIX1G pyroxenite (55) and 9% of the chemical composition of dolomite (MgO = 21.86 wt % and CaO = 30.41 wt %; excluding CO_2) and then normalized to 100%. The assumed melting pressure is 3 GPa. We plot the estimated residual modal abundances and CaO and CaO/Al_2O_3 values of the melts produced by 0–40% melting of the mixed lithology and the MIX1G pyroxenite in *SI Appendix*, Fig. S7. Results show that the addition of CaO to a pyroxenitic source increases the modal proportion of clinopyroxene at the expense of garnet (*SI Appendix*, Fig. S7*A*), but this has little effect on the CaO content and CaO/Al_2O_3 ratio of partial melts formed from this assemblage (*SI Appendix*, Fig. S7 *B* and *C*).

Comparison Between Oceanic and Subcontinental EM1 Sources. The common element characterizing Pitcairn basalts and the intracontinental EM1 basalts is the involvement of an ancient, low-$\delta^{26}Mg$ EM1 component in their mantle sources. The difference between the two settings may lie in the mechanism and location of the decarbonation processes required to account for the low CaO/Al_2O_3 ratios characterizing all EM1 basalts. For Pitcairn basalts, decarbonation proceeded most likely through carbonate–silicate reactions during subduction of dolomite-bearing sediments, as explained above. Intracontinental EM1 sources, on the other hand, were more likely decarbonated in the transition zone through the loss of carbonatite melts in the presence of K-hollandite (22), to account for their exceptionally high K/U and Ba/Th ratios, as well as their positive Zr–Hf anomalies, features that distinguish the intracontinental EM1 basalts from Pitcairn basalts (*SI Appendix*, Fig. S8). In any case, in both settings the magnesium isotopes are the main carbonate memory left in the EM1 source, and neither scenario supports actual subduction of substantial amounts of carbonates into the lower mantle, at least not during late Archean or early Proterozoic time when the subduction zones were presumably hotter than in geologically more recent times (49).

Materials and Methods

Major Oxides, Trace Elements, and Radiogenic Isotopes. All rock samples were powdered in an alumina mill. Whole-rock geochemical compositions other than Mg isotopes were determined at the Japan Agency for Marine-Earth Science and Technology. Major and trace element compositions of whole-rock samples were analyzed by X-ray fluorescence spectrometry and inductively coupled plasma-quadrupole mass spectrometry (ICP-QMS). Pb, Sr, Nd, and Hf isotope ratios were measured on rock powders, after acid leaching, by thermal ionization mass spectrometry for Sr and Nd isotopes and multiple-collector ICP-MS for Pb and Hf isotopes. The detailed descriptions for sample preparation, chemical treatment, and analytical conditions are given in *SI Appendix*, *Part 1*.

Mg Isotopes. Mg isotope analyses were performed at the Institute of Geology and Geophysics, Chinese Academy of Sciences, following previously well-established procedures (58). All samples and US Geological Survey (USGS) rock reference materials were weighed in Savillex screw-top beakers and then digested by using concentrated acids in the following sequence: (*i*) HF-HNO_3 (3:2, vol/vol), (*ii*) HCl-HNO_3 (3:1, vol/vol), and (*iii*) HNO_3, until they were completely dissolved. The clear solutions were dried and dissolved in 2 mol/L HNO_3 to obtain Mg concentrations of 20 ppm. Mg purification was achieved by cation exchange chromatography in Savillex microcolumns loaded with 2 mL of Bio-Rad AG50W-X12 (38–74 μm) resin. Each sample solution containing 20 μg Mg was loaded onto the resin. The same column procedure was carried out twice to obtain pure Mg solutions. One or two synthetic Mg solutions (IGGMg1-A) and at least two USGS rock reference materials were processed through the same column procedure with our investigated samples for checking the column chemistry. Purified sample and standard solutions were diluted to 2 ppm Mg using the same batch of 2% HNO_3. After column chemistry, the Mg yields were ≥99.8% for all reference materials and unknown samples. The total procedural Mg blank during this study was less than 6 ng.

Mg isotopic compositions were measured by the sample–standard bracketing method on a Thermo Scientific Neptune MC-ICP-MS. A quartz dual cyclonic spray chamber combined with an Elemental Scientific Inc. 50 μL min^{-1} PFA MicroFlow Teflon nebulizer was used as the introduction system. Each sample was measured at least four times and then averaged. Mg isotopic compositions are expressed in δ notation as per mil (‰) deviation from DSM3: $\delta^X Mg = [(^X Mg/^{24}Mg)_{sample}/(^X Mg/^{24}Mg)_{DSM3} - 1] \times 1{,}000$, where X = 25 or 26. The

long-term external precision was determined by repeated analyses of the international standards (DSM3 and Cambridge 1), in-house Mg standards (IGG Mg1 and SRM980), and various rock reference materials, and this value is better than ±0.06‰ (2 SD) for δ^{26}Mg. Repeated measurements of the Cambridge 1 and IGG Mg1 at different dates yielded average δ^{26}Mg values of −2.62 ± 0.05‰ (2 SD, n = 26) and −1.75 ± 0.05‰ (2 SD, n = 34), respectively. Comparison between our results of standards/USGS rock reference materials and published values is summarized in Dataset S4. In a plot of δ^{25}Mg′ vs. δ^{26}Mg′ (*SI Appendix*, Fig. S9), all samples fall along the mass-dependent fractionation line for Mg isotopes.

The data supporting the findings of this study are available in either the *SI Appendix* or the published works cited.

ACKNOWLEDGMENTS. We thank J.-H. Yang, Y.-H. Yang, and C. Huang for their laboratory or technical support. We appreciate the highly constructive reviews from Matthew Jackson, Catherine Chauvel, and Paterno Castillo. This study was financially supported by the National Natural Science Foundation of China (Grants 41372064, 41688103, and 41672049), the Programme of Introducing Talents of Discipline to Universities of China (Grant B13021), and the Program A for Outstanding PhD Candidate of Nanjing University (Award 201701A005).

1. Hofmann AW (1997) Mantle geochemistry: The message from oceanic volcanism. *Nature* 385:219–229.
2. White WM (2015) Probing the earth's deep interior through geochemistry. *Geochem Perspect* 4:95–251.
3. Zindler A, Hart S (1986) Chemical geodynamics. *Annu Rev Earth Planet Sci* 14:493–571.
4. Woodhead JD, McCulloch MT (1989) Ancient seafloor signals in Pitcairn Island lavas and evidence for large amplitude, small length-scale mantle heterogeneities. *Earth Planet Sci Lett* 94:257–273.
5. Chauvel C, Hofmann AW, Vidal P (1992) HIMU-EM: The French Polynesian connection. *Earth Planet Sci Lett* 110:99–119.
6. Eisele J, et al. (2002) The role of sediment recycling in EM-1 inferred from Os, Pb, Hf, Nd, Sr isotope and trace element systematics of the Pitcairn hotspot. *Earth Planet Sci Lett* 196:197–212.
7. Delavault H, Chauvel C, Thomassot E, Devey CW, Dazas B (2016) Sulfur and lead isotopic evidence of relic Archean sediments in the Pitcairn mantle plume. *Proc Natl Acad Sci USA* 113:12952–12956.
8. Gasperini D, et al. (2000) Evidence from Sardinian basalt geochemistry for recycling of plume heads into the Earth's mantle. *Nature* 408:701–704.
9. Willbold M, Stracke A (2010) Formation of enriched mantle components by recycling of upper and lower continental crust. *Chem Geol* 276:188–197.
10. McKenzie D, O'Nions RK (1983) Mantle reservoirs and ocean island basalts. *Nature* 301:229–231.
11. Castillo PR (2017) An alternative explanation for the Hf-Nd mantle array. *Sci Bull (Beijing)* 62:974–975.
12. Wombacher F, et al. (2011) Magnesium stable isotope fractionation in marine biogenic calcite and aragonite. *Geochim Cosmochim Acta* 75:5797–5818.
13. Hofmann AW, White WM (1982) Mantle plumes from ancient oceanic crust. *Earth Planet Sci Lett* 57:421–436.
14. Jackson MG, et al. (2007) The return of subducted continental crust in Samoan lavas. *Nature* 448:684–687.
15. White WM, Hofmann AW (1982) Sr and Nd isotope geochemistry of oceanic basalts and mantle evolution. *Nature* 296:821–825.
16. Zhong Y, et al. (2017) Magnesium isotopic variation of oceanic island basalts generated by partial melting and crustal recycling. *Earth Planet Sci Lett* 463:127–135.
17. French SW, Romanowicz B (2015) Broad plumes rooted at the base of the Earth's mantle beneath major hotspots. *Nature* 525:95–99.
18. Duncan RA, McDougall I, Carter RM, Coombs DS (1974) Pitcairn Island-another Pacific hot spot? *Nature* 251:679–682.
19. Hanyu T, et al. (2011) Geochemical characteristics and origin of the HIMU reservoir: A possible mantle plume source in the lower mantle. *Geochem Geophys Geosyst* 12:Q0AC09.
20. Lai YJ, et al. (2015) The influence of melt infiltration on the Li and Mg isotopic composition of the Horoman Peridotite Massif. *Geochim Cosmochim Acta* 164:318–332.
21. Teng FZ (2017) Magnesium isotope geochemistry. *Rev Mineral Geochem* 82:219–287.
22. Wang XJ, et al. (2017) Mantle transition zone-derived EM1 component beneath NE China: Geochemical evidence from Cenozoic potassic basalts. *Earth Planet Sci Lett* 465:16–28.
23. Tian HC, et al. (2016) Origin of low δ^{26}Mg basalts with EM-I component: Evidence for interaction between enriched lithosphere and carbonated asthenosphere. *Geochim Cosmochim Acta* 188:93–105.
24. Jackson MG, Dasgupta R (2008) Compositions of HIMU, EM1, and EM2 from global trends between radiogenic isotopes and major elements in ocean island basalts. *Earth Planet Sci Lett* 276:175–186.
25. Pilson MEQ (2013) *An Introduction to the Chemistry of the Sea* (Cambridge Univ Press, Cambridge), 2nd Ed, p 67.
26. Teng FZ, Wadhwa M, Helz RT (2007) Investigation of magnesium isotope fractionation during basalt differentiation: Implications for a chondritic composition of the terrestrial mantle. *Earth Planet Sci Lett* 261:84–92.
27. Chen LM, et al. (2018) Magnesium isotopic evidence for chemical disequilibrium among cumulus minerals in layered mafic intrusion. *Earth Planet Sci Lett* 487:74–83.
28. Wang SJ, Teng FZ, Scott JM (2016) Tracing the origin of continental HIMU-like intraplate volcanism using magnesium isotope systematics. *Geochim Cosmochim Acta* 185:78–87.
29. Wang SJ, Teng FZ, Rudnick RL, Li SG (2015) Magnesium isotope evidence for a recycled origin of cratonic eclogites. *Geology* 43:1071–1074.
30. Schulze DJ (1989) Constraints on the abundance of eclogite in the upper mantle. *J Geophys Res* 94:4205–4212.
31. Jacob DE (2004) Nature and origin of eclogite xenoliths from kimberlites. *Lithos* 77:295–316.
32. Aulbach S, Viljoen KS (2015) Eclogite xenoliths from the Lace kimberlite, Kaapvaal craton: From convecting mantle source to palaeo-ocean floor and back. *Earth Planet Sci Lett* 431:274–286.
33. Gale A, et al. (2013) The mean composition of ocean ridge basalts. *Geochem Geophys Geosyst* 14:489–518.
34. Yang W, et al. (2016) Magnesium isotopic composition of the deep continental crust. *Am Mineral* 100:243–252.
35. Huang J, et al. (2015) Magnesium isotopic compositions of altered oceanic basalts and gabbros from IODP site 1256 at the East Pacific Rise. *Lithos* 231:53–61.
36. Su BX, et al. (2015) Iron and magnesium isotope fractionation in oceanic lithosphere and sub-arc mantle: Perspectives from ophiolites. *Earth Planet Sci Lett* 430:523–532.
37. Wang SJ, Teng FZ, Rudnick RL, Li SG (2015) The behavior of magnesium isotopes in low-grade metamorphosed mudrocks. *Geochim Cosmochim Acta* 165:435–448.
38. Veizer J, Hoefs J, Lowe DR, Thurston PC (1989) Geochemistry of Precambrian carbonates: II. Archean greenstone belts and Archean sea water. *Geochim Cosmochim Acta* 53:859–871.
39. Shields G, Veizer J (2002) Precambrian marine carbonate isotope database: Version 1.1. *Geochem Geophys Geosyst* 3:1–12.
40. Sumner DY, Beukes NJ (2006) Sequence stratigraphic development of the Neoarchean Transvaal carbonate platform, Kaapvaal Craton, South Africa. *S Afr J Geol* 109:11–22.
41. Beukes NJ (1987) Facies relations, depositional environments and diagenesis in a major early Proterozoic stromatolitic carbonate platform to basinal sequence, Campbellrand Subgroup, Transvaal Supergroup, Southern Africa. *Sediment Geol* 54:1–46.
42. Garapić G, et al. (2015) A radiogenic isotopic (He-Sr-Nd-Pb-Os) study of lavas from the Pitcairn hotspot: Implications for the origin of EM-1 (enriched mantle 1). *Lithos* 228–229:1–11.
43. Castillo PR (2015) The recycling of marine carbonates and sources of HIMU and FOZO ocean island basalts. *Lithos* 216–217:254–263.
44. Dasgupta R, Hirschmann MM, Stalker K (2006) Immiscible transition from carbonate-rich to silicate-rich melts in the 3 GPa melting interval of eclogite + CO_2 and genesis of silica-undersaturated ocean island lavas. *J Petrol* 47:647–671.
45. Dasgupta R, Hirschmann MM, Smith ND (2007) Partial melting experiments of peridotite + CO_2 at 3 GPa and genesis of alkalic ocean island basalts. *J Petrol* 48:2093–2124.
46. Scott JM, Turnbull IM, Auer A, Palin JM (2013) The sub-Antarctic Antipodes volcano: A <0.5 Ma HIMU-like Surtseyan volcanic outpost on the edge of the Campbell Plateau, New Zealand. *New Zeal J Geol Geop* 56:134–153.
47. Sobolev AV, Hofmann AW, Nikogosian IK (2000) Recycled oceanic crust observed in 'ghost plagioclase' within the source of Mauna Loa lavas. *Nature* 404:986–990.
48. Herzberg C, et al. (2014) Phantom Archean crust in Mangaia hotspot lavas and the meaning of heterogeneous mantle. *Earth Planet Sci Lett* 396:97–106.
49. Dasgupta R (2013) Ingassing, storage, and outgassing of terrestrial carbon through geologic time. *Rev Mineral Geochem* 75:183–229.
50. Grassi D, Schmidt MW (2011) The melting of carbonated pelites from 70 to 700 km depth. *J Petrol* 52:765–789.
51. Wyllie PJ, Huang WL, Otto J, Byrnes AP (1983) Carbonation of peridotites and decarbonation of siliceous dolomites represented in the system CaO-MgO-SiO_2-CO_2 to 30 kbar. *Tectonophysics* 100:359–388.
52. Kakizawa S, Inoue T, Suenami H, Kikegawa T (2015) Decarbonation and melting in $MgCO_3$–SiO_2 system at high temperature and high pressure. *J Mineral Petrol Sci* 110:179–188.
53. Martin AM, Hammouda T (2011) Role of iron and reducing conditions on the stability of dolomite + coesite between 4.25 and 6 GPa–A potential mechanism for diamond formation during subduction. *Eur J Mineral* 23:5–16.
54. Porter KA, White WM (2009) Deep mantle subduction flux. *Geochem Geophys Geosyst* 10:Q12016.
55. Hirschmann MM, Kogiso T, Baker MB, Stolper EM (2003) Alkalic magmas generated by partial melting of garnet pyroxenite. *Geology* 31:481–484.
56. Pertermann M, Hirschmann MM (2003) Anhydrous partial melting experiments on MORB-like eclogite: Phase relations, phase compositions and mineral–melt partitioning of major elements at 2–3 GPa. *J Petrol* 44:2173–2201.
57. Ghiorso MS, Hirschmann MM, Reiners PW, Kress VC (2002) The pMELTS: A revision of MELTS for improved calculation of phase relations and major element partitioning related to partial melting of the mantle to 3 GPa. *Geochem Geophys Geosyst* 3:1–35.
58. An YJ, et al. (2014) High-precision Mg isotope analyses of low-Mg rocks by MC-ICP-MS. *Chem Geol* 390:9–21.
59. Teng FZ, et al. (2010) Magnesium isotopic composition of the Earth and chondrites. *Geochim Cosmochim Acta* 74:4150–4166.